

Structural studies of poly(*p*-phenylene selenide) doped with sulphur trioxide

W. CZERWIŃSKI, L. KREJA

Institute of Chemistry, N. Copernicus University, 87-100 Toruń, Poland

P. HRUSZKA, J. JURGA

Polymer Processing Laboratory, Technical University of Poznań, ul. Piotrowo 3, 60-965 Poznań, Poland

B. BRYCKI

Department of Chemistry, A. Mickiewicz University, ul. Grunwaldzka 6, 60-780 Poznań, Poland

Poly(*p*-phenylene selenide) (PPSe) was prepared by condensation polymerization of 2,4 dibromobenzene and sodium selenide. The synthesis product in the form of powder was purified. The structure of the resulting polymer was investigated by infrared spectroscopy, wide-angle X-ray spectroscopy, electron diffraction, ultraviolet, electron spin resonance and elemental analysis. ¹H-nuclear magnetic resonance (NMR) solid measurements were used to determine the molecular dynamics for undoped and SO₃-doped PPSe. The NMR investigations for undoped PPSe have shown that there are no essential differences in the structure and molecular motion between PPSe and PPS. After doping PPSe with SO₃, contrary to PPS, a third component of relaxation time, *T*₁, is observed. The relaxation times for this component are connected to the interaction of protons with paramagnetic centres which are generated as a result of the doping process. The electrical conductivity of SO₃-doped PPSe at the beginning of the doping process rapidly increased to about $6 \times 10^{-6} \text{ S cm}^{-1}$ and then decreased more than one order of magnitude because of the chemical reaction which had occurred.

1. Introduction

In recent years, conducting polymers with a non-degenerate ground state have attracted strong interest. Various conjugated polymers exist which belong to this group, such as poly(*p*-phenylene) (PPP), poly(pyrrole) (PPy), poly(thiophene) (PT), poly(*p*-phenylene sulphide) (PPS), etc. Polaron-type defects in these polymers have been theoretically predicted [1] and experimentally verified [2]. The transport properties of the neutral form of these compounds are mainly related to the band gap which is rather significant.

Conjugated polymers can be chemically or electrochemically doped to reach metallic conductivities. The ionization potential and electron affinity values determine the capability of these polymers for oxidative (p-type) or reductive (n-type) doping.

One polymer with a non-degenerate ground state is poly(*p*-phenylene selenide) (PPSe) which has been only investigated up to now to a small extent [3-6]. Moreover, investigation on the nuclear magnetic resonance (NMR) in solid PPSe has not been reported to date.

It is known [7], that PPS doped by strong p-dopant molecules has a rather high conductivity ($\sim 1 \text{ S cm}^{-1}$) but during the doping process the chemical structure of the polymer is changed, resulting in at least one new

(PBT) polymer. Substitution of sulphur by selenium in poly(*p*-phenylene chalcogenide) chains may be favourable in an electronic sense, due to the increased metallic character of selenium and its smaller electronegativity. Moreover, there is experimental evidence that doped selenium molecular compounds have higher conductivities than similar sulphur systems and better electrical properties at low temperatures [8, 9]. On the other hand, contrary results were reported when a heavier chalcogen (Se) was used to produce the chalcogen-containing polymers [3, 5].

In the present work we investigated ¹H-NMR solid in undoped and SO₃-doped PPSe and compared these results with PPS. It is known from the literature [10, 11] that the resonance lines in PPS have a two-component character above the glass temperature. The two-phase behaviour of a polymer is usually associated with the presence of at least two regions which differ in the degree of chain motion. The narrow component of the resonance line is, in general, characteristic of amorphous domains, and the broad component corresponds to crystalline region present in semicrystalline PPS. The temperature dependences of *T*₁ and *T*_{1g} have shown that at low temperature the relaxation process is due to the interaction between protons and paramagnetic centres [11]. At higher

temperatures the relaxation is described by the dipolar interaction which is in line with the rotations of the phenyl rings around the sulphur–phenyl–sulphur axis [10, 11].

2. Experimental procedure

Poly(*p*-phenylene selenide) (PPSe) was synthesized from *p*-dibromobenzene and sodium selenide in the presence of NMP and a flow of argon at high temperature (393–413 K) for 20 h.

All reagents used in the synthesis were especially purified, and the solvent was distilled directly before the reaction was performed. After extraction of oligomers, the product in powder form was vacuum dried at 368 K.

¹H-NMR experiments were performed for undoped and SO₃-doped PPSe. In both cases, polymer in the form of powder was degassed to eliminate remaining oxygen and moisture ($p = 10^{-5}$ torr (1 torr = 133.322 Pa), temperature 373 K, time 24 h). The doping process was carried out in a special chamber under a pressure of SO₃- vapour of about 80 torr. During the doping procedure, the colour changed from beige to black. Under the same conditions, the pressed pellets (396 MPa) of PPSe and PPS (commercial product) were doped to measure the electrical conductivity using the two-contact electrodes method.

Fourier transform-infrared wide-angle X-ray, electron diffraction, ultraviolet-visual, electron spin resonance studies and elemental analysis methods were also used to characterize the physico-chemical structure of the investigated materials.

In the ¹H-NMR experiments, the linewidth and relaxation times, T_1 , as functions of temperature for undoped and doped PPSe were investigated. The linewidth measurements were made on a spectrometer with self-acting stabilization on H₁ and a frequency of 30 MHz [12]. The relaxation time measurements were made using a pulse-spectrometer [13] with a frequency of 30 MHz using the $\pi/2 - \tau - \pi/2$ method. The pulse width was 2 μ s and the dead-time of the spectrometer was 10 μ s.

3. Results and discussion

3.1. Elemental analysis

The composition (as obtained from chemical analysis) of the PPSe after extraction of oligomers and the drying procedure, is given in Table I. Chemical analysis of the pure product showed a small percentage of bromine which is located on the end of the chains.

TABLE I The composition of PPSe after extraction of oligomers (obtained from elemental analysis)

	C	H	Se	Br	Purity (%)
Found	45.17	2.64	48.50	3.04	99.75
Calculated	46.47	2.60	50.93	–	

The bromine content, assuming that all chains have terminal bromine groups, gave the possibility of calculating the average degree of polymerization (DP) and the molecular weight (MW) which are, in this case, 33 and 5278, respectively.

Elemental analysis of PPSe corresponds to (C_{6.0}H_{4.2}Se_{0.99}Br_{0.03}) and showed that no diselenide linkages were present in the chain of PPSe and the product was of high purity.

3.2. Infrared studies

Fourier transform-infrared (FT-IR) spectra of the pure and SO₃-doped poly(*p*-phenylene selenide) are shown in Fig. 1. The spectrum of the undoped PPSe displays the characteristic triad at high energies (1565, 1471 and 1379 cm⁻¹) which is attributed to the ring stretching vibrations. The out-of-plane vibrations of the two paired hydrogen atoms in the phenyl ring at 814 cm⁻¹ indicate the para substitution of the phenyl ring. The presence of the typical bands for *p*-phenylene polymers at 1005 and 474 cm⁻¹ [14] as well as the carbon–selenide stretching vibration at 500 cm⁻¹ also confirm the proposed structure for poly(*p*-phenylene selenide). The absence of diselenide linkages near 285 cm⁻¹ detected in separate experiments, is consistent with the result of elemental analysis which showed a stoichiometric C:Se ratio. The infrared spectrum of the undoped PPSe is very similar to that of PPS [14, 15] except for the C–Se stretching vibration band which is shifted to lower frequencies according to the mass effect and reduced electronegativity of selenium in comparison to sulphur.

The FT-IR spectrum of SO₃-doped PPSe shows significant changes in comparison to that of the undoped sample. The characteristic feature of this spectrum is a broad absorption at 3700–2500 cm⁻¹, which is due to the hydrogen-bonded OH groups undoubtedly coming from SO₂–OH groups. The presence of these groups upon doping with SO₃ is strongly evinced by the appearance of a band at 1176 cm⁻¹, which is assigned to the asymmetric stretching vibrations of SO₃H groups, as well as a new band at 851 cm⁻¹, which is due to the out-of-plane vibrations of the isolated hydrogen in the phenyl ring. The low intensity of these bands and small changes in the other bands indicate that the main part of PPSe remains unchanged upon doping with SO₃.

The enhanced conductivity of PPSe doped with SO₃ is a result of the formation of the other adducts. However, the concentration of these adducts is too low to be detected by infrared spectroscopy.

3.3. Ultraviolet-visible (UV-VIS) spectroscopy

The electronic spectrum of PPSe shown in Fig. 2 exhibits a broad absorption band with the edge near 3.5 eV and a maximum about 4.1 eV (3400 cm⁻¹), with the tail into the visible accounting for the colour of the polymer. The broad peak near 4.1 eV is assignable to a low-energy $\pi \rightarrow \pi^*$ transition and is characteristic of the optical energy gap of PPSe.

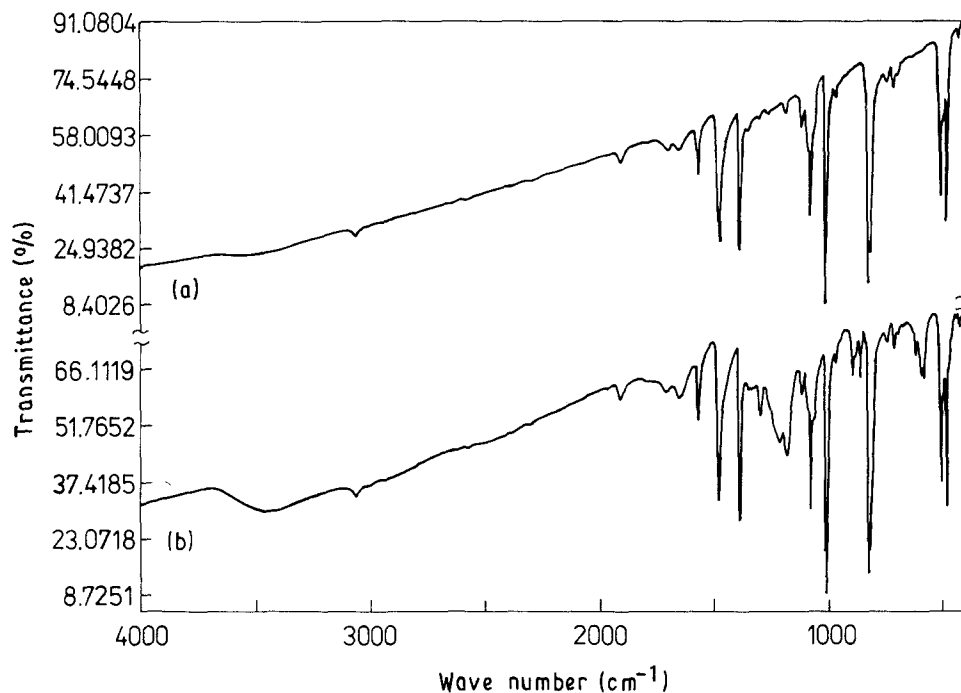


Figure 1 FT-IR spectra of PPS: (a) undoped, (b) doped with SO_3 .

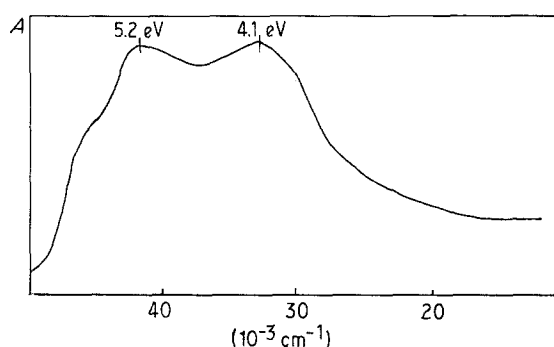


Figure 2 Electronic spectra of undoped PPS.

3.4. Wide-angle X-ray (WAXS) and electron diffraction (ED) studies

The X-ray diffraction pattern of pure (without oligomers) PPS powder shown in Fig. 3 reveals partial crystallinity and a structure isomorphous to that reported [16] for PPS. The strongest peak is observed at $2\theta = 20.3^\circ$ with the shift compared to PPS, to larger d -value in line with the increasing Van der Waal's radius of selenium compared to sulphur. The crystallite size (coherence length) calculated from the Sherrer equation for the strongest (1 1 1) crystalline reflection is 14.5 nm. The intensity of the residual Bragg peaks was too small to calculate the crystallite size with sufficient accuracy.

The electron diffraction patterns of pure PPS, and PPS for comparison, are plotted in Fig. 4. It can be clearly seen that some narrow Bragg reflections exist, but the d -spacing in the case of PPS is a little larger than in the case of PPS. For the strongest Bragg peaks (1 1 1) for PPS, this d -value is 0.428 nm and for PPS 0.431 nm. The d -spacing for the (1 1 0) Bragg reflection is 0.469 nm for PPS and 0.479 nm for PPS. Other peaks for PPS also show a shift to a larger d -value compared to PPS.

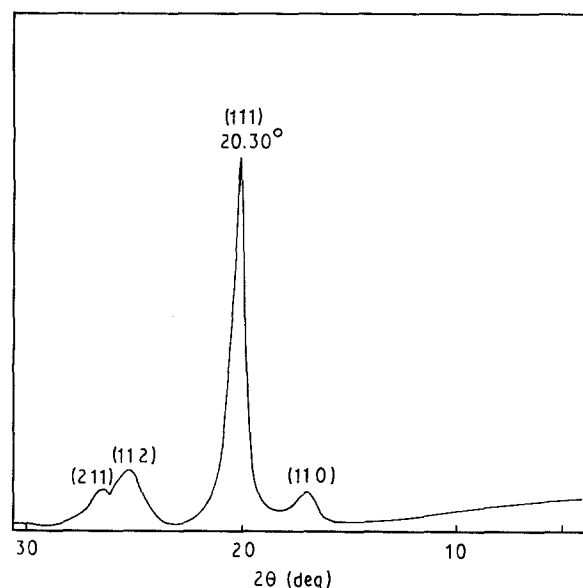


Figure 3 X-ray diffraction pattern for undoped PPS.

After exposure to SO_3 the original reflections become broader and partially disappear. The doped PPS sample showed a diffraction pattern typical of a rather amorphous material. This indicates that at least SO_3 molecules penetrate the whole structure of PPS and not only the amorphous part present in the semicrystalline polymer. This phenomenon is known for aryl polymers and was described [17] for a PPS doped with AsF_5 vapour.

The X-ray and electron diffraction data suggest that PPS analogous to PPS crystallizes in the orthorhombic system with two fragments of chain per unit cell.

3.5. Electron spin resonance (ESR) study

The ESR preliminary study (300 K) on undoped PPS indicated that the concentration of free spins was

about $8.25 \times 10^{15} \text{ spin g}^{-1}$ and peak-to-peak distance linewidth was about 5.1 G. Only one symmetrical line of a Lorentzian shape was observed for the undoped polymer. The g -value was 2.0030, very close to the value of free electrons.

3.6. Electrical conductivity

In Fig. 5 the electrical conductivity as a function of doping time of SO_3 is plotted for PPSe and PPS, respectively. The maximum electrical conductivity for PPSe is about $6 \times 10^{-6} \text{ Scm}^{-1}$ and is almost two orders of magnitude smaller than in the case of doped PPS under the same conditions.

Moreover, during exposure to SO_3 vapour the electrical conductivity for PPS increased in the initial

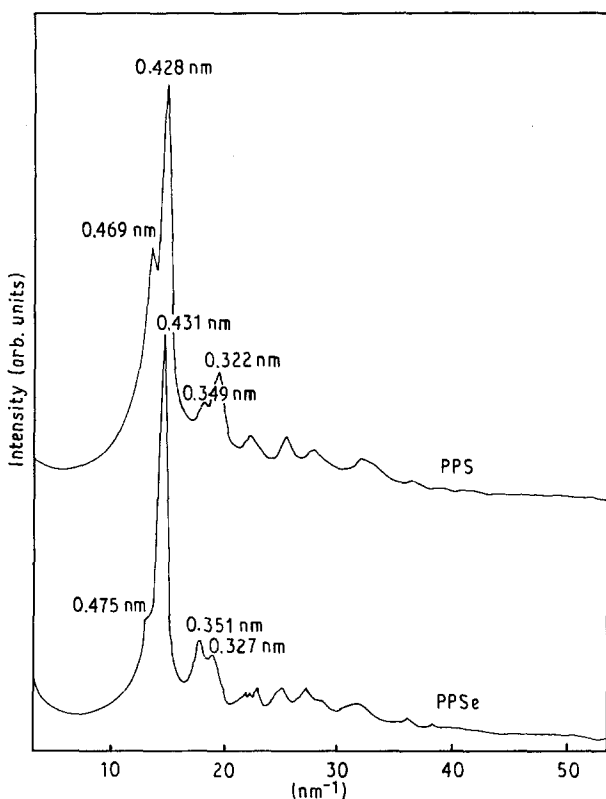


Figure 4 Electron diffraction pattern for PPSe and PPS.

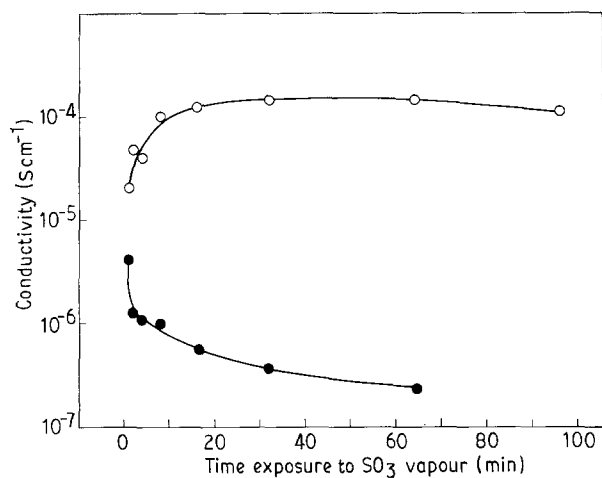


Figure 5 Electrical conductivity of PPSe and PPS doped with SO_3 , ($p_{\text{SO}_3} = 80 \text{ torr}$). (○) PPS, (●) PPSe.

stage of the doping process, whereas for PPSe the electrical conductivity decreased by more than one order of magnitude after exposure to SO_3 for more than 1 h. It is known [18] that doping of PPSe with strong acceptor agents (AsF_5 , SO_3) produces a compound with a low electrical conductivity which decreases during the doping process. It is probably the result of chemical reactions between the backbone of chain and acceptor molecules, as confirmed by the infrared spectrum given above.

3.6.1. $^1\text{H-NMR}$ study of undoped PPSe

In Fig. 6 the shape of the NMR line is shown for PPSe at low and high temperatures. At low temperatures only a single line of linewidth about 7.5 G exists which is characteristic for the rigid structure of PPSe. Above 280 K this single line becomes a two-component line, as for other semicrystalline polymers above the glass transition.

The narrow line of linewidth 1 G is connected with the amorphous part of polymer, and the broad-component line with the crystalline phase of a semicrystalline polymer. At higher temperatures ($> 480 \text{ K}$) the broad line disappears because of the melting of the crystalline phase. The melting temperature of PPSe measured by DTA is 490 K [5].

In Fig. 7, the temperature dependence of linewidth for both components is given. The dependence is similar to that observed in PPS and the linewidth for the rigid phase is the same in both PPS and PPSe [11]. In the range 220–380 K, a gradual decrease in the broad-component linewidth is observed, due to the molecular reorientation process. The energy of activation of this process is described by [19]

$$\ln(1/W - 1/A) = -E_A/kT + \ln(1/B - 1/A) \quad (1)$$

where W is the linewidth at temperature T , A and B are constant values of linewidth at low and high temperatures, respectively, E_A is the activation energy.

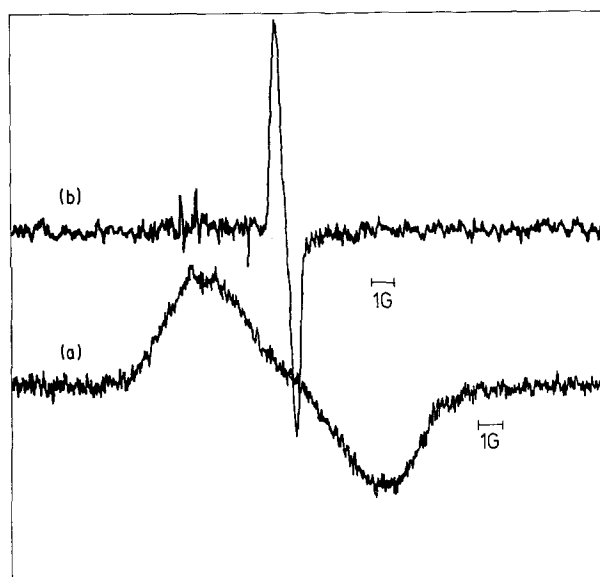


Figure 6 $^1\text{H-NMR}$ lines in PPSe, (a) 120 K, (b) 500 K.

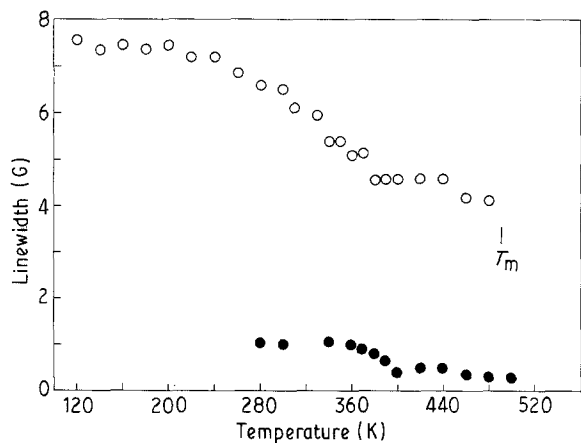


Figure 7 The temperature dependence of linewidth for PPSe.

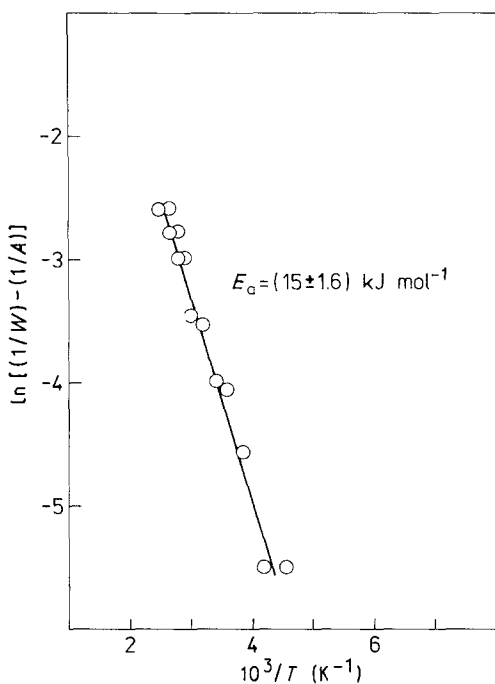


Figure 8 The linewidth as a function of T^{-1} for PPSe, related to Equation 1.

Fig. 8 shows a plot of temperature dependence of the linewidth for PPSe in the range 220–380 K. The thermal activation energy of molecular rearrangement is $15 \pm 1.6 \text{ kJ mol}^{-1}$ and is only slightly higher than for PPS ($14 \pm 1.0 \text{ kJ mol}^{-1}$ [11]). In the case of PPS this energy was ascribed to a rotation of phenyl rings in the crystalline phase [11]. However, from our calculations of the proton interaction energy in the crystalline phase of PPS, it was found that free rotation of phenyl rings was impossible [20]. Therefore, the narrowing line in PPSe may be assigned, as in PPS, to the hindered rotation of phenyl rings in crystalline regions of the polymer. It is possible that full free rotation may exist in the amorphous phase or at least at high temperatures (melt), before decomposition of the material.

3.6.1.1. Relaxation time, T_1 . Magnetization recovery in PPSe was non-exponential over the full range of temperatures. Fig. 9 shows an example of this depend-

ence on time at 120 K. The dependence may be shown with high accuracy, c.c. = 0.9998, as a sum of two-components. The fraction of the component of longer relaxation time is independent of temperature and is equal to 85%. The temperature dependence of relaxation time is shown in Fig. 10. The shape of this dependence indicates that analogous to PPS [11], two basis relaxation mechanisms exist in PPSe. At high temperatures dipolar relaxation dominates; at temperatures below $T_{1 \text{ min}}$ temperature the relaxation rate may be written as

$$1/T_1' = c_1 \exp(-E_A/kT) \quad (2)$$

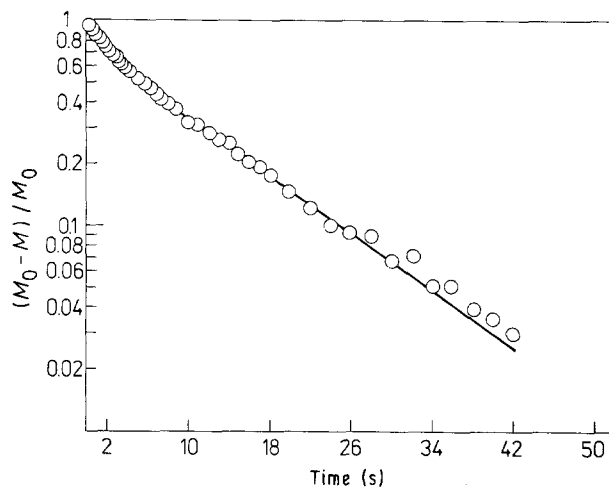


Figure 9 The magnetization recovery as a function of time for PPSe at 120 K. (—) Fitting of experimental points for a two-component relaxation time.

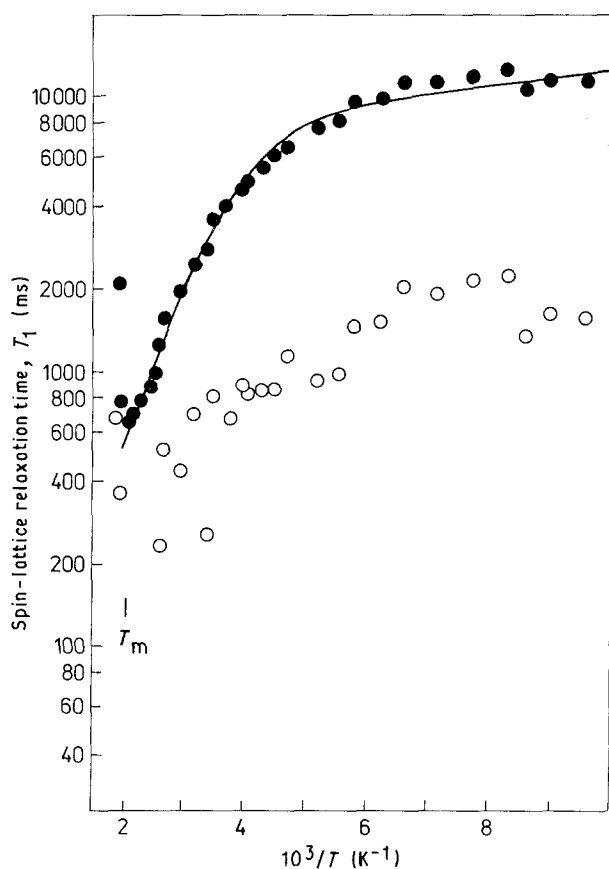


Figure 10 (○) Relaxation time spin-lattice T_1 as a function of T^{-1} for undoped PPSe. (—●—) Calculated from Equations 2 and 3 for parameters given in text.

In the low-temperatures range the main relaxation mechanism is connected with interaction of protons with paramagnetic centres, which is proved by the small influence of temperature on T_1 . The presence of these centres is also found from ESR investigations.

The paramagnetic relaxation rate is given by

$$1/T_1'' = c_2 \exp(-E_p/kT) \quad (3)$$

The total relaxation rate may be presented as an expression which is the sum of Equations 2 and 3.

The experimental points of the longer T_1 component were fitted to this expression. Relatively good fit was obtained for following parameters: $c_1 = 44 \text{ s}^{-1}$, $E_A = 13 \text{ kJ mol}^{-1}$, $c_2 = 0.16 \text{ s}^{-1}$, $E_p = 0.6 \text{ kJ mol}^{-1}$. It is represented by the full line in Fig. 10.

The activation energy of molecular movements characteristic for dipolar relaxation ($13 \pm 2.6 \text{ kJ mol}^{-1}$) is in line with E_A calculated from the temperature dependence of linewidth, and is the same order as in PPS [11]. It is pointed out that dipolar relaxation is associated with the hindered rotation of phenyl rings in the crystalline phase of the polymer. The dramatic increase in relaxation time above 480 K indicates the phase transition due to melting of the crystalline region of PPSe. At the same temperature, the broad-component of the resonance line disappears.

The scatter of experimental points for the short-component (Fig. 10) is higher than for the long-component of T_1 . This is caused by the small fraction of this component in the total relaxation process, 15%, and therefore, a low accuracy in the case of the short-component is obtained.

The temperature dependence for a short-component is smaller than for a long one. This may indicate that the dipolar relaxation related to this component of T_1 is induced by molecular movements with a lower activation energy. It may also reflect that in the molecular region typical for a short-time component, the concentration of paramagnetic centres is higher than in the region described by a long-time component.

It is fulfilled for both processes assuming that the short-time component is related to the amorphous phase of the polymer.

Non-identical relaxation times, T_1 , for amorphous and crystalline regions in PPSe, indicate that there is no spin diffusion between both phases. This is contrary to the results of PPS, where identical relaxation times for both regions were detected [11, 12]. Considerably higher values of the long T_1 component in PPSe indicate a lower concentration of paramagnetic centres in our material, compared to PPS [11, 12].

3.6.2. $^1\text{H-NMR}$ in SO_3 -doped PPSe

3.6.2.1. NMR linewidth. The NMR investigations of SO_3 -doped PPSe were made only in the low temperature range, because above 300 K a redoping process occurs. In Fig. 11 the temperature dependence of NMR linewidth for doped PPSe is shown. The linewidth is practically constant up to room temperature, indicating that the rotation of phenyl rings in the

crystalline phase of the polymer is completely hindered by the doping molecules. Moreover, as a result of the doping process, the NMR line becomes narrower by about 0.5 G, compared to the undoped sample. Thus the interactions between protons are a little weaker as a result of chain separation by the SO_3 molecules.

3.6.2.2. Relaxation time, T_1 . Magnetization recoveries in doped samples of PPSe are non-exponential over the whole temperature range. This is clearly seen in Fig. 12 where the magnetization recovery at 120 K is shown. Interpretation of this magnetization recovery in the framework of the two-component relaxation time was unsuccessful because of insufficient accuracy. So the expression

$$\exp[-(t/T_1)^{1/2}] \quad (4)$$

was applied, which is related to relaxation through paramagnetic centres without spin diffusion. The fitting of the experimental points to the above expression was fulfilled only in a very limited region. The best fit gives three components of T_1 . The proton fractions corresponding to these components are: for the short one 15%, for the medium one 45% and for the long one 40%. The temperature dependence for all

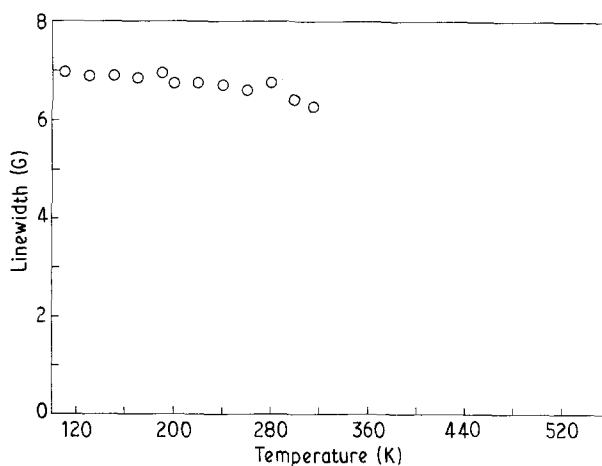


Figure 11 The temperature dependence of NMR linewidth for PPSe doped with SO_3 .

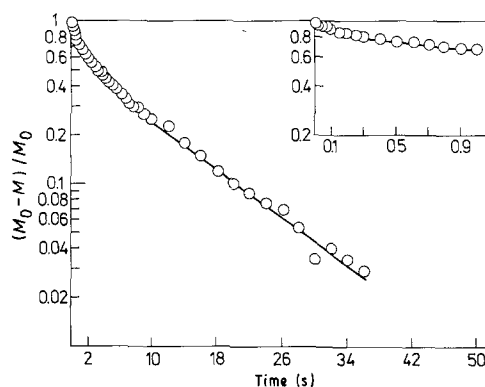


Figure 12 The magnetization recovery as a function of time at 120 K. (—) Fitting procedure for three-component relaxation times.

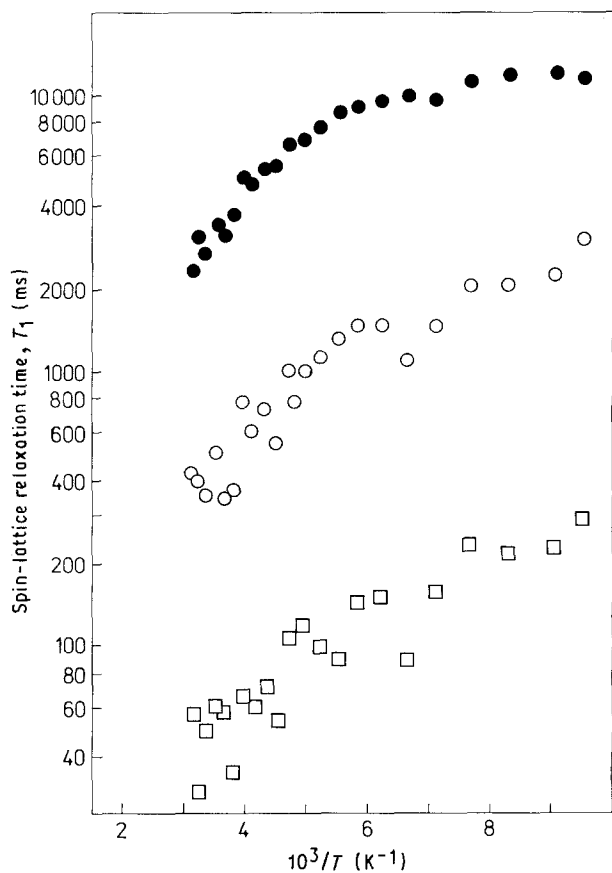


Figure 13 The dependence of spin-lattice T_1 relaxation time on T^{-1} for PPSe doped with SO_3 . (●) Long, (○) medium, (□) short components, respectively.

T_1 components in doped PPSe are given in Fig. 13. The values of medium and long T_1 components are the same as those of the undoped sample. Thus approximately 85% of the polymer remains undoped and relaxation proceeds in the same way as in the undoped PPSe. However, the short-component of T_1 is much lower for doped than undoped PPSe. This is the result of the increased concentration of paramagnetic centres in the effectively doped part of the polymer. Such a phenomenon has already been observed in PPS doped with SO_3 [22].

4. Conclusions

Resonance lines in PPSe as well as in PPS are two-component at elevated temperatures. The broad component corresponds to the crystalline phase and the narrow one to the amorphous phase. The linewidths for the crystalline phases of both polymers are identical at low temperatures, which confirms the suggestions given by Acampora *et al.* [5] about the isomorphism of crystalline PPSe and PPS.

The temperature dependence of linewidth in PPSe is similar to that observed in PPS. The activation energy in the high-temperature range is of the same order for both polymers and is connected with hindered rotation of phenyl rings in the crystalline phase of the polymer. The melting point of that phase obtained from broad-line measurements is close to that observed by the DTA method. It is lower by about 70 K than for PPS.

The magnetization recovery in T_1 relaxation time measurements for PPSe is non-exponential over the whole temperature range and may be considered a two-component dependence. On the other hand, in PPS the relaxation is mono-exponential due to rapid spin diffusion between amorphous and crystalline phases. The existence of two relaxation times in PPSe may reflect the fact that spin exchange between the phases is restricted, compared to PPS. The temperature dependence of relaxation times for PPSe is similar to that of PPS.

Two relaxation mechanisms were found in PPSe, analogous to PPS. At high temperatures, dipolar relaxation dominates which is caused by hindered rotation of phenyl rings. At low temperatures the relaxation is connected with interaction of protons with paramagnetic centres, the presence of which was confirmed by ESR. Considerably longer relaxation times at low temperatures in PPSe in comparison to PPS may indicate a lower concentration of paramagnetic centres.

NMR measurements which were made for pure PPSe show that there is no essential difference between structure and molecular dynamics in PPS and PPSe.

The doping of PPSe with SO_3 showed that electrical conductivity increased, but its value was two orders of magnitude lower than for PPS doped under the same conditions. The decreasing conductivity during the doping process corresponds to the chemical reaction between SO_3 and the backbone of chains, which was confirmed by infrared spectroscopy. The SO_3 molecules penetrate the whole volume of the polymer yielding, as a result, an almost amorphous structure.

The linewidth is slightly narrower for doped PPSe at lower temperatures compared to the undoped sample. Over the whole range of temperatures the linewidth is almost constant; this may reflect total hindered rotation of phenyl rings by penetrating molecules. As a result of the doping process, the third component of T_1 occurs with a participation of 15%. The values of relaxation time for third component indicate that this component is due to the relaxation process between protons and paramagnetic centres generated by SO_3 -molecules, analogous to PPS.

On the other hand, elemental analysis showed that in a doped sample there was almost 20% sulphur atoms, which corresponds well with the results of nuclear relaxation measurements.

References

1. J. L. BREDAS, B. THEMANS, J. G. FRIPIAT and J. M. ANDRE, *Phys. Rev. B* **29** (1984) 6761.
2. J. FINK, B. SCHEERER, M. STAMM, B. TIEKE, B. KANELLAKOPOULOS and E. DORNBERGER, *Phys. Rev. B Rapid Commun.* **30** (1984) 4867.
3. S. TANAKA, M. SATO, K. KAERIYAMA, H. KANETSUNA, M. KATO and Y. SUDA, *Makromol. Chem. Rapid Commun.* **4** (1983) 231.
4. D. J. SANDMAN, M. RUBNER and L. SAMUELSON, *J. Chem. Soc. Chem. Commun.* (1982) 1133.
5. L. A. ACAMPORA, D. L. DRUGGER, T. EMMA, J. MOHAMMED, M. F. RUBNER, L. SAMUELSON,

- D. J. SANDMAN and S. K. TRIPATHY, ASC Symposium Series 242 (1984) "Polymer in Electronics", edited by (Theodore Davidson (Amer. Chem. Soc., 1984) p. 461.
6. W. CZERWIŃSKI, J. FINK and N. NUCKER, "Electronic Properties of Conjugated Polymers" (Springer, Berlin, 1987) p. 330.
 7. R. L. ELSENBAUMER, L. W. SHACKLETTE, J. M. SOWA and R. H. BAUGHMAN, *Molec. Cryst. Liq. Cryst.* **83** (1982) 229.
 8. J. H. PERLSTEIN, *Angew. Chem. Int. Ed. Engl.* **16** (1977) 519.
 9. E. M. ENGLER and V. V. PATEL, *J. Amer. Chem. Soc.* **96** (1974) 7376.
 10. J. JURGA, H. ECKERT and W. MULLER-WARMUTH, *Z. Naturforsch.* **34a** (1979) 1216.
 11. S. SCHLICK and B. R. MCGARVEY, *Polym. Commun.* **25** (1984) 369.
 12. J. JURGA, *Sci. Instrum.* **3** (1988) 67.
 13. J. JURGA and K. JURGA, *ibid.* **4** (1989) 23.
 14. D. O. HUMMEL and F. SCHOLL, "Atlas der Polymer und Kunststoffanalyse" (Carl Hanser, Munchen, 1978).
 15. S. KAZAMA, K. ARAI and E. MAEKAWA, *Synth. Met.* **15** (1986) 299.
 16. K. F. SCHOCH Jr, J. F. CHANCE and K. E. PFEIFFER, *Macromol.* **18** (1985) 2389.
 17. N. S. MURTHY, R. L. ELSENBAUMER, J. E. FROMMER and R. H. BAUGHMAN, *Synth. Met.* **9** (1984) 91.
 18. K. Y. JEN, M. V. LAKSHMIKANTHAM, M. ALBECK, M. P. CAVA, W. S. HUANG and A. G. McDIARMID, *J. Polym. Sci. Polym. Lett. Ed.* **21** (1983) 441.
 19. J. R. HENDRICKSON, P. J. BRAY, *J. Magn. Reson.* **9** (1973) 341.
 20. J. JURGA, to be published.
 21. D. TSE and S. R. HARTMANN, *Phys. Rev. Lett.* **21** (1968) 511.
 22. S. KAZAMA, *Synth. Met.* **16** (1986) 77.

*Received 31 August 1990
and accepted 28 February 1991*